Temperature-Dependent Spectrum of an Antiferroelectric Linear Chain Model*

B. D. SILVERMAN
Raytheon Company Research Division, Waltham, Massachusetts
(Received April 12, 1962)

Some general properties of the lattice vibrational spectra of antiferroelectric materials with the perovskite structure are illustrated with the use of a simple model. It is shown that electrostatic interactions can contribute significantly to the observed difference between the Curie temperature and the transition temperature. The temperature dependence of transverse and longitudinal branches is exhibited.

I. INTRODUCTION

THE relationship between the transition to a ferroelectric state and the lattice vibrational spectrum of crystals having the perovskite structure has been discussed by Cochran[1] and others[2,3]. It has been suggested that this transition is the result of an instability of a certain infrared active vibrational mode. At the transition temperature the frequency of this mode goes to zero and the ions then seek new positions of equilibrium. On the low-temperature side of the transition, the ionic displacements from the cubic state are similar to the displacements associated with the mode which becomes unstable. The crystal is polar[4] in the low-temperature phase. In the nonpolar or cubic state, the temperature dependence of this infrared active frequency is held responsible for the Curie-Weiss behavior of the static dielectric constant. Recently, Barker and Tinkham[5] have observed a low-lying transverse optical frequency by measurements of the reflectivity of strontium titanate at liquid air and room temperatures. The frequency at these two temperatures agrees quite well with the proposed temperature dependence

$$\omega \sim (T-T_C)^{1/2}. \tag{1.1}$$

The dispersion of the dielectric constant was also shown to be a resonant type and not a relaxation type. This work strongly substantiates the suggested intimate relation between the Curie-Weiss behavior of the dielectric constant and the temperature dependence of this soft infrared active frequency. Similar measurements performed on the other well-known perovskite ferroelectrics, e.g., $BaTiO_3$, $PbTiO_3$, and $KNbO_3$ would be instructive.

Cochran[1] has suggested that a transition to an antiferroelectric state can also be considered the result of an instability of a lattice vibrational mode. The ionic displacements associated with this mode would yield a nonpolar structure. Several antiferroelectric materials having the perovskite structure are known,[6] e.g., $PbZrO_3$,[7] $PbHfO_3$,[8] and $NaNbO_3$.[9,10] Above the antiferroelectric transition temperature, these materials are paraelectric and exhibit a dielectric constant which obeys a Curie-Weiss law. Their Curie constants are on the order of the Curie constants of the ferroelectric perovskites previously mentioned. Their Curie temperatures (obtained from the high-temperature dielectric behavior) are lower than the temperatures at which they become antiferroelectric. This behavior suggests that these antiferroelectric materials also have associated with them, an infrared active frequency whose temperature dependence is given by Eq. (1.1). It appears that before the temperature is lowered to a value for which this long-wavelength mode would become unstable, another mode with wavelength on the order of the lattice parameter becomes unstable, hence resulting in an antiferroelectric transition.

Since the energies of various dipolar configurations arrived at by small structural perturbations from the cubic state are very close, the dispersion introduced into the transverse optical branch by the long-range electrostatic interactions is small. With neglect of any dispersion due to the short-range forces, a low frequency at $k=0$ would imply the existence of low frequencies over the entire branch. It is therefore reasonable that the "antiferroelectric mode" belongs to the same branch as does the infrared active soft mode. It is of interest to determine whether the observed difference between the Curie temperature and the transition temperature can be accounted for by the dispersion introduced into the transverse branch by the electrostatic interactions. Using a simple model as a basis for investigation, it will be shown that electrostatic interactions can indeed contribute significantly to the difference between the two

* Work supported, in part, by the Electronics Research Directorate of the Air Force Cambridge Research Center, Air Research and Development Command.

[1] W. Cochran, Phys. Rev. Letters **3**, 412 (1959); in *Advances in Physics*, edited by N. F. Mott (Taylor and Francis, Ltd., London, 1960), Vol. 9, p. 387; in *Advances in Physics*, edited by N. F. Mott (Taylor and Francis, Ltd., London, 1961), Vol. 10, p. 401.

[2] P. W. Anderson, paper given at *All-Union Conference on Dielectrics, Moscow, 1958* (Bull. Acad. Sci. USSR, 1960), Vol. 24.

[3] R. Landauer, H. Juretschke, and P. Sorokin (unpublished report).

[4] In what follows, the problem of domain formation will be neglected.

[5] A. S. Barker, Jr., and M. Tinkham, Phys. Rev. **125**, 1527 (1962).

[6] Two excellent review articles concerning ferroelectricity and antiferroelectricity and containing extensive references up through 1956 are W. Kanzig, in *Solid State Physics*, edited by F. Seitz and D. Turnbull (Academic Press Inc., New York, 1957), Vol. 4, p. 1. P. W. Forsbergh, Jr., in *Handbuch der Physik*, edited by S. Flügge (Springer-Verlag, Berlin, 1956), Vol. 17.

[7] G. Shirane, E. Sawaguchi, and Y. Takagi, J. Phys. Soc. Japan **6**, 208 (1951); S. Roberts, J. Am. Ceram. Soc. **33**, 63 (1950).

[8] G. Shirane and R. Pepinsky, Phys. Rev. **91**, 812 (1953).

[9] L. E. Cross, Phil. Mag. [8] **1**, 76 (1956).

[10] G. Shirane, R. Newnham, and R. Pepinsky, Phys. Rev. **96**, 581 (1954).

aforementioned temperatures. The problem of determining the relative stability of states for actual materials must therefore include an analysis of the relative stability of various dipolar configurations. There have been attempts[11–13] to determine the most stable dipolar configuration of $BaTiO_3$ from electrostatic considerations. The results are, however, inconclusive for several reasons. The relative stability of only a few configurations has been tested. Subsequent x-ray and neutron diffraction studies[14] on $BaTiO_3$ have suggested a configuration different from those tested. It has been shown recently by Kurosawa[15] that the effective charges for the ions of a few ferroelectric perovskites are reduced to one-fourth or one-fifth of the purely ionic values. It is questionable whether the effects of this charge reduction can be treated within the framework of an ionic-type model. The short-range forces should be known in some detail before predictions for the actual crystal can be made. Since ferroelectric and antiferroelectric configurations are so close in energy, a slight wave-vector dependence of the short-range forces could drastically modify the results based on only a consideration of the long-range forces.

In view of this complexity, we will restrict the investigation to the properties of simple model with the intent of providing some insight concerning the dielectric properties and lattice vibrational spectra of the antiferroelectric perovskites.

II. MODEL

The model that will be investigated in this paper has been treated elsewhere in connection with the microwave loss in $SrTiO_3$.[16] All oxygen ions are coupled by a spring of constant K to their nearest-neighbor cations (Fig. 1). These are the cations which are at the center of the oxygen octahedra. The ionic charges of cation and anion are taken to be equal in magnitude and opposite in sign. Charge neutrality is obtained for the system by distributing the charge of the cation at the cell corner (twice the charge of the cation in the center of the oxygen octahedron) uniformily over the unit cell. The only other role of these A cations (formula unit ABO_2) is to constrain the oxygen movement to be perpendicular to the unit cell face on which the oxygen atom lies. It is apparent that with neglect of electrostatic interactions this model is composed of three uncoupled sets of O-B chains. The directions of the chains are [100], [010], and [001]. A longitudinal mode of vibration with propagation vector along the [100] direction will involve only displacements of the atoms belonging to the chains which lie along this direction. A transverse mode with the same propagation vector will involve ionic displacements along the chains lying in either the [010] or [001] direction. For simplicity the masses of cation and anion are chosen equal. This can be generalized simply and would result in the treatment of a diatomic linear chain instead of a monatomic chain. The electronic polarizabilities of cation and anion are chosen equal. This is necessary to stabilize the simple system that has been described.

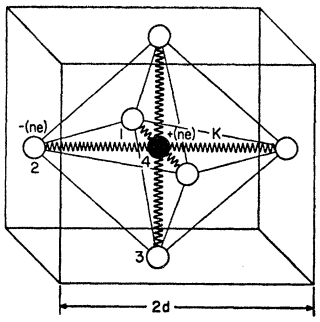

FIG. 1. Unit cell of chain model.

The frequency spectrum of this model will be investigated as a function of temperature for the [100] direction of propagation. The model will be shown to be essentially a model of an antiferroelectric, i.e., an instability will develop due to the vanishing of the frequency at the edge of the zone. Since the frequency spectrum of the transverse optical branch is flat in the absence of electrostatic forces, the effect of these forces on the dispersion of this branch can be seen directly. The dispersion of this branch is a measure of the difference between the Curie temperature and the temperature of the antiferroelectric transition.

First, we investigate the vibrational spectrum with neglect of the electrostatic forces. The effect of introducing the long-range forces will then be discussed in connection with the temperature dependence of the spectrum. The four inequivalent atoms of the unit cell are labeled in Fig. 1. The equation of motion for the κth ion with neglect of the electronic polarizability is written in the notation of Kellerman[17] (see Appendix).

$$m\omega^2 U_{\kappa x}+\sum_{\kappa',y}\begin{bmatrix}\kappa & \kappa'\\ x & y\end{bmatrix}U_{\kappa' y}-\sum_{\kappa',y}\begin{bmatrix}\kappa & \kappa'\\ x & y\end{bmatrix}_{k=0}U_{\kappa y}=0. \quad (2.1)$$

The first term is the inertial term. The second term arises from the x component of the force on the κth ion due to the displacements of all other ions in the lattice. The third term arises from the x component of the force on the κth ion due to its displacement from equilibrium while the other atoms are held fixed. For propagation along the x or [100] direction the equations of motion

[11] M. H. Cohen, Phys. Rev. **84**, 369 (1951).
[12] Y. Takagi, *Proceedings of the International Conference on Theoretical Physics, Kyoto and Tokyo, September, 1953* (Science Council of Japan, Tokyo, 1954), p. 824.
[13] W. Kinase, Progr. Theoret. Phys. Japan **13**, 529 (1955).
[14] H. T. Evans, Massachusetts Institute of Technology Laboratory Insulation Research Technical Report, No. 58, 1953 (unpublished); B. C. Frazer, H. Danner, and R. Pepinsky, Phys. Rev. **100**, 745 (1955); G. Shirane, R. Pepinsky, and B. C. Frazer, *ibid.* **97**, 1175 (1955); G. Shirane, H. Danner, and R. Pepinsky, *ibid.* **105**, 856 (1957).
[15] T. Kurosawa, J. Phys. Soc. Japan **16**, 1298 (1961).
[16] B. D. Silverman, Phys. Rev. **125**, 1921 (1962).
[17] E. W. Kellerman, Phil. Trans. Roy. Soc. **238**, 513 (1940).

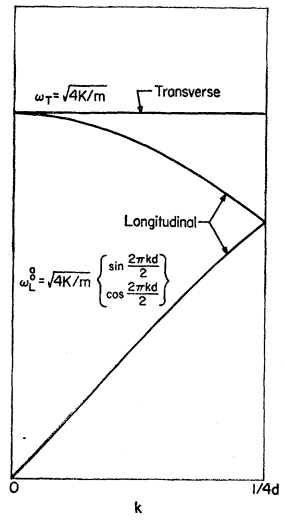

FIG. 2. Spectrum with neglect of the electrostatic forces.

are

$$\left\{m\omega^2+\begin{bmatrix}4 & 4\\ x & x\end{bmatrix}-\begin{bmatrix}4 & 4\\ x & x\end{bmatrix}_{k=0}-\begin{bmatrix}4 & 1\\ x & x\end{bmatrix}_{k=0}\right\}U_{4x}+\begin{bmatrix}4 & 1\\ x & x\end{bmatrix}U_{1x}=0, \tag{2.2}$$

$$\begin{bmatrix}4 & 1\\ x & x\end{bmatrix}U_{4x}+\left\{m\omega^2+\begin{bmatrix}4 & 4\\ x & x\end{bmatrix}-\begin{bmatrix}4 & 4\\ x & x\end{bmatrix}_{k=0}-\begin{bmatrix}4 & 1\\ x & x\end{bmatrix}_{k=0}\right\}U_{1x}=0, \tag{2.3}$$

$$\left\{m\omega^2+\begin{bmatrix}4 & 4\\ y & y\end{bmatrix}-\begin{bmatrix}4 & 4\\ y & y\end{bmatrix}_{k=0}-\begin{bmatrix}4 & 2\\ y & y\end{bmatrix}_{k=0}\right\}U_{4y}+\begin{bmatrix}4 & 2\\ y & y\end{bmatrix}U_{2y}=0, \tag{2.4}$$

$$\begin{bmatrix}4 & 2\\ y & y\end{bmatrix}U_{4y}+\left\{m\omega^2+\begin{bmatrix}4 & 4\\ y & y\end{bmatrix}-\begin{bmatrix}4 & 4\\ y & y\end{bmatrix}_{k=0}-\begin{bmatrix}4 & 2\\ y & y\end{bmatrix}_{k=0}\right\}U_{2y}=0. \tag{2.5}$$

Equations (2.2) and (2.3) determine the vibrational spectrum of the longitudinal modes. Considering only the short-range spring constant coupling described, we write

$$\begin{bmatrix}4 & 4\\ x & x\end{bmatrix}^R=0;\quad\begin{bmatrix}4 & 1\\ x & x\end{bmatrix}^R=2K\cos 2\pi kd;\quad 0\leq k\leq 1/4d. \tag{2.6}$$

The longitudinal frequencies are, therefore,

$$\omega_L^2(k)=(2K/m)[1\pm\cos 2\pi kd]. \tag{2.7}$$

This is just the spectrum for a linear monatomic chain. This result should be obvious from the model without resorting to the preceding analysis. The formal analysis is given however to facilitate the presentation of the more complete calculation, i.e., with electrostatic interactions included.

Equations (2.4) and (2.5) determine the vibrational spectrum of the transverse modes. The coupling parameters are

$$\begin{bmatrix}4 & 4\\ y & y\end{bmatrix}^R=0;\quad\begin{bmatrix}4 & 2\\ y & y\end{bmatrix}^R=2K, \tag{2.8}$$

and the transverse optical frequencies are

$$\omega_T^2=4K/m. \tag{2.9}$$

The frequencies of the transverse branch exhibit no dispersion and are all equal to the $k=0$ longitudinal optical frequency [Eq. (2.7)]. The frequency spectrum is shown in Fig. 2. The frequencies of the transverse acoustic branch are all identically equal to zero. This is indicative of the instability of the model against a shearing force. This unnatural feature of the model does not concern us since we are interested in the internal strains[18] and not homogeneous deformations of the model. The transverse optical branch is flat since a change in wavelength for this branch specifies only a change in phase of the motion of one chain with respect to another, and there is no coupling between the chains. When the electrostatic interactions are taken into account, this branch will exhibit dispersion since the long-range forces on the ions are different for different phasings of the chains.

III. TEMPERATURE-DEPENDENT SPECTRUM

The transverse optical frequency will now be obtained with the inclusion of the electrostatic forces. The cation equation of motion for a transverse mode with propagation vector in the [100] direction and ionic displacements along the [010] direction is [using Eq. (A26)]

$$m\omega^2U_{4y}+2KU_{2y}-2KU_{4y}+\frac{g}{g(k)}\times\left\{\begin{bmatrix}4 & 2\\ y & y\end{bmatrix}^C U_{2y}+\begin{bmatrix}4 & 4\\ y & y\end{bmatrix}^C U_{4y}-\begin{bmatrix}4 & 2\\ y & y\end{bmatrix}^C_{k=0}U_{4y}-\begin{bmatrix}4 & 4\\ y & y\end{bmatrix}^C_{k=0}U_{4y}\right\}=0, \tag{3.1}$$

with

$$g=\left[1-\frac{\alpha}{q^2}\left(\begin{bmatrix}4 & 4\\ y & y\end{bmatrix}^C_{k=0}+\begin{bmatrix}4 & 2\\ y & y\end{bmatrix}^C_{k=0}\right)\right], \tag{3.2}$$

$$g(k)=\left[1+\frac{\alpha}{q^2}\left(\begin{bmatrix}4 & 2\\ y & y\end{bmatrix}^C-\begin{bmatrix}4 & 4\\ y & y\end{bmatrix}^C\right)\right]. \tag{3.3}$$

[18] M. Born and K. Huang, *Dynamical Theory of Crystal Lattices* (Oxford University Press, New York, 1954), Chap. III.

The g functions represent the modification of the equations of motion due to the presence of ions which are electronically polarizable. For the transverse optical branch of the chain model we have (since anions and and cations are equivalent except for the sign of their ionic charge)

$$U_{4y}=-U_{2y}, \tag{3.4}$$

and therefore

$$\omega_T^2(k)=\frac{1}{m}\left[4K+\frac{g}{g(k)}\left\{\begin{bmatrix}4 & 4\\ y & y\end{bmatrix}^C_{k=0}+\begin{bmatrix}4 & 2\\ y & y\end{bmatrix}^C_{k=0}-\begin{bmatrix}4 & 4\\ y & y\end{bmatrix}^C+\begin{bmatrix}4 & 2\\ y & y\end{bmatrix}^C\right\}\right]. \tag{3.5}$$

If we define

$$a(k)=\begin{bmatrix}4 & 4\\ y & y\end{bmatrix}^C_{k=0}+\begin{bmatrix}4 & 2\\ y & y\end{bmatrix}^C_{k=0}-\begin{bmatrix}4 & 4\\ y & y\end{bmatrix}^C+\begin{bmatrix}4 & 2\\ y & y\end{bmatrix}^C, \tag{3.6}$$

then

$$\omega_T^2(k)=\frac{1}{m}\left[4K+\frac{g}{g(k)}a(k)\right]. \tag{3.7}$$

The $[\ ]^C$ are obtained by performing dipolar sums over the lattice. These sums have been performed for the chain model by using the well-known Ewald-theta transformation (see reference 17). Both sums, i.e., the sums over real and reciprocal space, are rapidly convergent for $k\neq 0$. To avoid the added complication of specifying boundary conditions for lattice waves with wavelength approaching the sample, we consider only modes with wavelength small compared with the sample size. A transverse optical mode of this type with wavelength large compared with the lattice parameter has a zero depolarization factor associated with it. A corresponding longitudinal mode of this type has the usual $-4\pi P$ depolarization factor associated with it. In this work we have collectively labeled all such modes as having zero wave vector.

The second term in the brackets of Eq. (3.7) arises from the electrostatic forces. This term is negative and is the "driving" force for a transition to the ferroelectric or antiferroelectric state. The Curie-Weiss behavior of the dielectric constant is assured if the $k=0$ transverse optical frequency has the following temperature dependence:

$$\omega_T^2(0)\sim(T-T_C). \tag{3.8}$$

T is the absolute temperature and T_C a constant to be identified with the Curie temperature. To obtain the temperature dependence appearing in Eq. (3.8) we will assume a slight linear temperature dependence of the spring constant K of the following form.

$$4K=-[g/g(0)]a(0)[1+c(T-T_C)]. \tag{3.9}$$

The constant c which is introduced here will be determined empirically. The $k=0$ transverse optical frequency can then be written

$$\omega_T^2(0)=-(1/m)[g/g(0)]a(0)c(T-T_C). \tag{3.10}$$

The origin of the slight temperature dependence of the spring constant can be considered to result from the effects of fourth-order anharmonic interactions on the spring constant of the linear theory.[19,20] The effect of such temperature-dependent spring constant on the frequency spectrum, however, is the same as any wave-vector independent term linear in temperature appearing in Eq. (3.7) regardless of its origin.

Substituting Eq. (3.9) into (3.7), we obtain the temperature-dependent frequency for each mode of the transverse branch

$$\omega_T^2(k)=-\frac{1}{m}\frac{g}{g(0)}a(0)c[T-(T_C+\Delta T_k)], \tag{3.11}$$

with

$$\Delta T_k=-\frac{1}{c}\left[\frac{g(0)a(k)-a(0)g(k)}{g(k)a(0)}\right]. \tag{3.12}$$

Each mode has associated with it an instability temperature $T_C+\Delta T_k$, the temperature at which the kth mode becomes unstable in the harmonic approximation. The preceding analysis no longer holds after the first mode becomes unstable since the ions move to new equilibrium positions. An analysis of the vibrational spectrum is then obtained by considering small displacements about the new equilibrium positions. The first mode to become unstable is the mode with the the largest positive ΔT_k. If no positive ΔT_k exists for any mode of wave vector k, the crystal will make a transition to the ferroelectric state at a temperature equal to T_C. For the model under consideration, it will be shown that the mode at the edge of the zone has the largest ΔT_k associated with it. The system will make a transition to an antiferroelectric state at a temperature $T_C+T_{k=1/4d}$.

The spectrum can be plotted as a function of temperature if the electronic polarizability α per unit volume, and the temperature coefficient c are known. These can be determined from a knowledge of the optical index of refraction in the paraelectric state and the Curie constant of the material under consideration. We will plot the spectrum to within a scale factor by using the observed properties of $PbZrO_3$. The Curie temperature T_C is obtained from the high temperature dielectric measurements on $PbZrO_3$.[7] The $a(k)$ [Eq. (3.6)] are dependent only on the effective charge and volume of the unit cell through a factor which cancels in the expression for ΔT_k. To calculate the $g(k)$ [Eq. (3.3)] it is necessary to specify the electronic polarizability per unit volume ($\alpha/8d^3$). To calculate ΔT_k it is necessary

[19] A. F. Devonshire, Phil. Mag. **40**, 1040 (1949).
[20] J. C. Slater, Phys. Rev. **78**, 748 (1950).

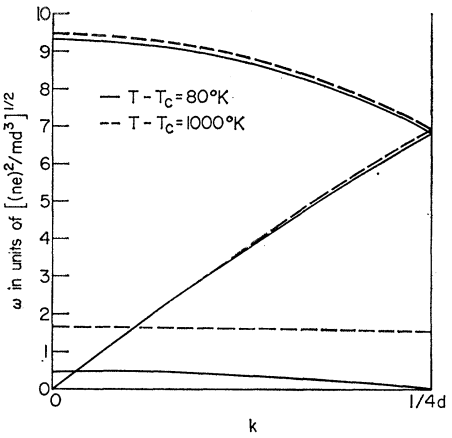

FIG. 3. Temperature-dependent spectrum.

to specify c, the temperature coefficient of the spring constant. These two quantities, $(\alpha/8d^3)$ and c will be determined, respectively, from the observed optical index of refraction and Curie constant[7] of $PbZrO_3$.

The dielectric constant of the chain model can be written

$$\epsilon=1+\frac{\pi\alpha}{d^3g(0)}+\frac{\pi}{cd^3g(0)}\left\{\alpha-\frac{g(0)(ne)^2}{2\begin{bmatrix}4 & 2\\ y & y\end{bmatrix}_0^c}\right\}\frac{1}{(T-T_C)}. \tag{3.13}$$

The square of the optical index of refraction is just the first two terms of Eq. (3.13):

$$\epsilon_\infty=1+\pi\alpha/d^3g(0). \tag{3.14}$$

Using Eqs. (3.3) and (3.14), we obtain

$$\frac{\alpha}{d^3}=\frac{1}{\pi}\frac{(\epsilon_\infty-1)}{[1+(\epsilon_\infty-1)(\frac{1}{2}q+\frac{1}{3})]}, \tag{3.15}$$

where

$$\begin{bmatrix}4 & 2\\ y & y\end{bmatrix}_0^c=-\frac{(ne)^2}{d^3}\frac{\pi}{2}(q+\tfrac{1}{3});\quad \begin{bmatrix}4 & 4\\ y & y\end{bmatrix}_0^c=\frac{(ne)^2}{d^3}\frac{\pi}{6}. \tag{3.16}$$

(Note: the same q appears in references 13 and 20.)

The ratio α/d^3 can be obtained by specifying ϵ_∞. To this author's knowledge the optical index of refraction of $PbZrO_3$ has only been reported for room temperature, where the material has been found to be orthorhombic.[21,22] The largest optical index of refraction along one of the principal directions has been chosen:

$$(\epsilon_\infty)^{1/2}=2.2 \quad \text{or} \quad \epsilon_\infty=4.84. \tag{3.17}$$

The qualitative features to be discussed are essentially insensitive to a more accurate choice of ϵ_∞.

[21] F. Jona, G. Shirane, and R. Pepinsky, Phys. Rev. **97**, 1584 (1955).

[22] E. Sawaguchi, H. Maniwa, and S. Hoshino, Phys. Rev. **83**, 1078 (1951).

Using $\epsilon_\infty=4.84$ and Eq. (3.15), we find

$$\alpha/d^3=0.178;\quad g(0)=0.144. \tag{3.18}$$

The temperature coefficient c can be determined from the value of the Curie constant C.

$$C=1.59\times10^5\ ^\circ\text{K}. \tag{3.19}$$

From Eqs. (3.13) and (3.16), we can write

$$c=\frac{\pi}{Cd^3g(0)}\left[\alpha+\frac{d^3g(0)}{\pi(q+\frac{1}{3})}\right], \tag{3.20}$$

and find

$$c=2.68\times10^{-5}\ ^\circ K^{-1}. \tag{3.21}$$

The Curie constant can be written, using Eq. (3.20),

$$C=\pi\alpha/cd^3g(0)+1/c(q+\tfrac{1}{3}). \tag{3.22}$$

The first term on the right is the contribution to the Curie constant from the electronic polarization. The second term is the contribution to the Curie constant from the lattice polarization. Looked at from this point of view, the lattice polarization contributes less than 10% to the value of the Curie constant. This indicates how important highly polarizable ions are, in contributing to the large dielectric constant of the perovskites in their paraelectric state. The temperature dependence of this electronic contribution arises from the temperature dependence of the local field at the sites of the electronic dipoles. The temperature dependence of the local field arises, in turn, from the temperature dependence of the lattice polarization and can be traced back to the temperature dependent spring constant.

The frequencies of the transverse optical branch [Eq. (3.11)] can now be plotted as a function of temperature to within a scale factor by using the values determined for α/d^3 and c [Eqs. (3.18) and (3.21)]. The temperature-dependent branch is shown in Fig. 3. Each frequency varies as the square root of the temperature minus an instability temperature. It is seen that the frequency of the mode at the edge of the zone goes to zero 80° above the temperature at which the uniform mode would become unstable. The transition temperature of $PbZrO_3$ is some 40° above its Curie temperature.[7] The difference in energies between ferroelectric and antiferroelectric dipolar configurations for the model yield a temperature difference between the states that is well within an order of magnitude of the observed value.[23] Figure 3 shows the entire branch to be temperature dependent. The temperature dependence at the edge of the zone reflects the development of the antiferroelectric instability. The temperature dependence at $k=0$ reflects the Curie-Weiss behavior of the dielectric constant.

[23] It should be mentioned that a mode at the edge of the zone with propagation vector k along one of the face diagonals of the unit cell is lower in energy than the mode at the edge of the zone that we have investigated. This mode which has associated with it displacements similar to the "checkerboard" configuration of Kinase becomes unstable 100° above the Curie temperature.

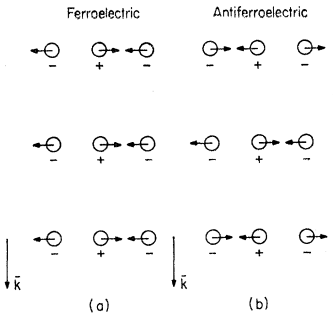

FIG. 4. Ionic displacements for ferroelectric and antiferroelectric modes.

Figure 4(b) shows the displacements of the atoms for the unstable mode. Segments of three horizontal chains are shown. This type of antiferroelectric configuration is similar to the "stripes" type of Kinase.[13] There is no net polarization since there is a polarization reversal in planes perpendicular to the propagation vector $\mathbf{k}$. In Fig. 4(a) the displacements of the atoms for the $k=0$ mode are shown. The origin of the instability can be understood essentially as follows. The central positive ion in diagram 4(a) experiences no net Coulomb force due to the neighboring positive ions shown (or from the entire positive ion lattice). The central positive ion in diagram 4(b) experiences a net force in the direction of its displacement due to the Coulomb repulsion of its positive neighbors. The instability at the edge of the zone can therefore be thought of as arising from the tendency of a plane of equivalent ions to buckle due to the mutual repulsion of like charges (if the charges are constrained so as not to have motion in the plane). This explanation is somewhat oversimplified since the $k=0$ mode is less stable if one considers only the interaction of the positive ion with the negative ions. For our model, however, this interaction is not sufficient to make the electrostatic energy of the ferroelectric state less than that of the antiferroelectric state.

The frequencies of the longitudinal acoustical and optical branches are

$$\omega_L^2(k)=\frac{1}{m}\left[2K(1\pm\cos 2\pi kd)+\frac{g}{g'(k)}a'(k)\right], \quad (3.23)$$

with

$$g=\left\{1-\frac{\alpha}{q^2}\left(\begin{bmatrix}4 & 4\\ x & x\end{bmatrix}^C_{k=0}+\begin{bmatrix}4 & 1\\ x & x\end{bmatrix}^C_{k=0}\right)\right\}$$

$$=\left\{1-\frac{\alpha}{q^2}\left(\begin{bmatrix}4 & 4\\ y & y\end{bmatrix}^C_{k=0}+\begin{bmatrix}4 & 2\\ y & y\end{bmatrix}^C_{k=0}\right)\right\}, \quad (3.24)$$

$$g'(k)=\left\{1+\frac{\alpha}{q^2}\left(\begin{bmatrix}4 & 1\\ x & x\end{bmatrix}^C-\begin{bmatrix}4 & 4\\ x & x\end{bmatrix}^C\right)\right\}, \quad (3.25)$$

$$a'(k)=\begin{bmatrix}4 & 4\\ x & x\end{bmatrix}^C_{k=0}+\begin{bmatrix}4 & 1\\ x & x\end{bmatrix}^C_{k=0}$$

$$-\begin{bmatrix}4 & 4\\ x & x\end{bmatrix}^C\pm\begin{bmatrix}4 & 1\\ x & x\end{bmatrix}^C. \quad (3.26)$$

The temperature-dependent longitudinal spectrum can be obtained by substitution of Eq. (3.9) into Eq. (3.23). In Fig. 3 the longitudinal optical and acoustical branches are shown. The frequencies have been plotted at two temperatures—the temperature of the antiferroelectric transition and 1000° above this. It is seen that over this large temperature interval the longitudinal branches are fairly temperature insensitive; the $k=0$ optical frequency varying by roughly 2% of its value. The transverse $k=0$ optical frequency, on the other hand, is strongly temperature dependent varying by roughly 300% of its low-temperature value. For the longitudinal motion, the depolarization contribution to the local field at the ionic sites acts as a long-range restoring force on the ions. No close cancellation of the harmonic driving and restoring forces occurs. The Lyddane-Sacks-Teller[24] relationship,

$$\omega_L^2(0)/\omega_T^2(0)=\epsilon_0/\epsilon_\infty, \quad (3.27)$$

relates the two optical frequencies at $k=0$ to the high- and low-frequency dielectric constants.

ACKNOWLEDGMENTS

I am indebted to L. Rimai for many interesting discussions. I would also like to thank Barbara Mikulec for the calculation of the dipolar sums.

APPENDIX

In this section, the equations of motion will be developed. The notation and procedure are similar to Kellerman's.[17] The differences, however, between Kellerman's equations of motion and the ones we will derive, arise since we treat a nondiagonally cubic structure in which the ions are polarizable.

The equilibrium position $\mathbf{r}_{0\kappa}{}^l$ of the κ, lth ion is

$$\mathbf{r}_{0\kappa}{}^l=\mathbf{a}^l+\mathbf{r}_{0\kappa}, \quad (A1)$$

where $\mathbf{a}^l=l_1\mathbf{a}_1+l_2\mathbf{a}_2+l_3\mathbf{a}_3$ defines the space lattice with basis vectors $\mathbf{r}_{0\kappa}$. The vectors $\mathbf{a}_1$, $\mathbf{a}_2$, $\mathbf{a}_3$ define the unit cell. The distance between the κ, lth ion and the κ', l'th ion is

$$\mathbf{r}_{0\kappa\kappa'}{}^{ll'}=\mathbf{r}_{0\kappa}{}^l-\mathbf{r}_{0\kappa'}{}^{l'}=\mathbf{a}^l-\mathbf{a}^{l'}+\mathbf{r}_{0\kappa}-\mathbf{r}_{0\kappa'}$$
$$=\mathbf{a}^{l-l'}+\mathbf{r}_{0\kappa}-\mathbf{r}_{0\kappa'}. \quad (A2)$$

Considering small independent displacements $\mathbf{u}_\kappa{}^l$ of each particle from its equilibrium position, the vector between the displaced particles is

$$\mathbf{r}_{\kappa\kappa'}{}^{ll'}=\mathbf{r}_{0\kappa\kappa'}{}^{l-l'}+\mathbf{u}_\kappa{}^l-\mathbf{u}_{\kappa'}{}^{l'}. \quad (A3)$$

Assuming only central forces, the total potential energy of the lattice is

$$\Phi=\tfrac{1}{2}\sum_{\kappa,\kappa'}\sum_{l,l'}\phi_{\kappa\kappa'}(|\mathbf{r}_{\kappa\kappa'}{}^{ll'}|). \quad (A4)$$

[24] R. H. Lyddane, R. G. Sachs, and E. Teller, Phys. Rev. **59**, 673 (1941).

The energy is developed in powers of the displacements. We consider the harmonic term

$$\Phi_2=-\tfrac{1}{2}\sum_{\kappa,\kappa'}\sum_{l,l'}\sum_{x,y}(\phi_{\kappa\kappa'}{}^{(l-l')})_{xy}u_{\kappa x}{}^{l}u_{\kappa' y}{}^{l'}$$
$$+\tfrac{1}{2}\sum_{\kappa,\kappa'}\sum_{l,l'}\sum_{x,y}(\phi_{\kappa\kappa'}{}^{(l-l')})_{xy}u_{\kappa x}{}^{l}u_{\kappa y}{}^{l}, \quad \text{(A5)}$$

where

$$(\phi_{\kappa\kappa'}{}^{l})_{xy}=\left[\frac{\partial^2}{\partial x\partial y}\phi_{\kappa\kappa'}(r)\right]_{r=r_{0\kappa\kappa' l}}. \quad \text{(A6)}$$

The equation for the x component of the motion of the κ, lth ion is

$$m_\kappa\ddot{u}_{\kappa x}{}^{l}-\sum_{\kappa',l',y}(\phi_{\kappa\kappa'}{}^{(l-l')})_{xy}u_{\kappa' y}{}^{l'}$$
$$+\sum_{\kappa',l',y}(\phi_{\kappa\kappa'}{}^{(l-l')})_{xy}u_{\kappa y}{}^{l}=0. \quad \text{(A7)}$$

Let us obtain the equations of motion for one Fourier component of the motion with frequency ω, wavelength λ, and wave vector $\mathbf{k}$. The displacements of the ions are then

$$\mathbf{u}_\kappa{}^{l}=\mathbf{U}_\kappa e^{-i\omega t}e^{2\pi i\mathbf{k}\cdot\mathbf{r}_{0\kappa l}};\quad |\mathbf{k}|=1/\lambda, \quad \text{(A8)}$$

and one finds

$$m_\kappa\omega^2U_{\kappa x}+\sum_{\kappa',y}\begin{bmatrix}\kappa & \kappa'\\ x & y\end{bmatrix}U_{\kappa' y}-\sum_{\kappa',y}\begin{bmatrix}\kappa & \kappa'\\ x & y\end{bmatrix}U_{\kappa y}=0, \quad \text{(A9)}$$

where we have defined

$$\begin{bmatrix}\kappa & \kappa'\\ x & y\end{bmatrix}=\sum_l(\phi_{\kappa'\kappa}{}^{l})_{xy}e^{2\pi i(\mathbf{k}\cdot\mathbf{r}_{\kappa'\kappa l})}. \quad \text{(A10)}$$

The forces on each ion are split up into a long-range contribution (Coulomb interaction) and a short-range repulsive part:

$$\begin{bmatrix}\kappa & \kappa'\\ x & y\end{bmatrix}=\begin{bmatrix}\kappa & \kappa'\\ x & y\end{bmatrix}^{C}+\begin{bmatrix}\kappa & \kappa'\\ x & y\end{bmatrix}^{R}. \quad \text{(A11)}$$

The Coulomb part is given by

$$\begin{bmatrix}\kappa & \kappa'\\ x & y\end{bmatrix}^{C}=q_\kappa q_{\kappa'}\sum_l\left[\frac{\partial^2}{\partial x\partial y}f(\mathbf{r}-\mathbf{a}^{l})\right]_{\mathbf{r}=\mathbf{r}_{0\kappa\kappa'}}$$
$$\times e^{2\pi i\mathbf{k}\cdot(\mathbf{a}^{l}-\mathbf{r}_{\kappa\kappa'})},\quad \kappa\neq\kappa', \quad \text{(A12)}$$

$$\begin{bmatrix}\kappa & \kappa\\ x & y\end{bmatrix}^{C}=q_\kappa{}^2\lim_{r\to0}\left[\sum_l\frac{\partial^2}{\partial x\partial y}f(\mathbf{r}-\mathbf{a}^{l})\right.$$
$$\left.\times e^{2\pi i\mathbf{k}\cdot\mathbf{a}^{l}}-\frac{\partial^2 f(\mathbf{r})}{\partial x\partial y}\right], \quad \text{(A13)}$$

with

$$f(\mathbf{r})=1/|\mathbf{r}|=1/r. \quad \text{(A14)}$$

The short-range repulsive part $\begin{bmatrix}\kappa & \kappa'\\ x & y\end{bmatrix}^{R}$ is given in Sec. III for the chain model [Eqs. (2.6) and (2.8)].

We will now obtain the equations of motion for the chain model with inclusion of the electronic polarizability α of the ions. The y component of the field at a point $\mathbf{r}$ due to the single electronic dipole $p_{\kappa' y}{}^{l'}$ at $\mathbf{r}_{\kappa'}{}^{l'}$ is

$$p_{\kappa' y}{}^{l'}\frac{\partial^2}{\partial y^2}\left[\frac{1}{|\mathbf{r}_{\kappa'}{}^{l'}-\mathbf{r}|}\right]. \quad \text{(A15)}$$

The field at the site $\mathbf{r}_\kappa{}^{l}$ due to all the dipoles is

$$\sum_{\kappa',l'\neq\kappa,l}p_{\kappa' y}{}^{l'}\left[\frac{\partial^2}{\partial y^2}\left(\frac{1}{r}\right)\right]_{r=r_{0\kappa'\kappa}{}^{l'l}}. \quad \text{(A16)}$$

The electronic moment at a site is proportional to the local field at that site.

$$p_{\kappa' y}{}^{l'}=\alpha E_{\kappa' y}{}^{l'}=\alpha Ee^{2\pi i\mathbf{k}\cdot\mathbf{r}_{0\kappa' l'}}. \quad \text{(A17)}$$

The field at $\mathbf{r}_{0\kappa}{}^{l}$ due to the surrounding electronic dipoles can then be written

$$\alpha E\sum_{\kappa',l'\neq\kappa,l}e^{2\pi i\mathbf{k}\cdot\mathbf{r}_{0\kappa' l'}}\left[\frac{\partial^2}{\partial y^2}\left(\frac{1}{r}\right)\right]_{r=r_{0\kappa'\kappa}{}^{l'l}}. \quad \text{(A18)}$$

The local field at the κ, lth site arises from the electronic dipoles and displaced ions.

$$E_{\kappa y}{}^{l}=Ee^{2\pi i\mathbf{k}\cdot\mathbf{r}_{0\kappa l}}$$
$$=\alpha E\sum_{\kappa',l'\neq\kappa,l}e^{2\pi i\mathbf{k}\cdot\mathbf{r}_{0\kappa' l'}}\left[\frac{\partial^2}{\partial y^2}\left(\frac{1}{r}\right)\right]_{r=r_{0\kappa'\kappa}{}^{l'l}}$$
$$+\sum_{\kappa',l'\neq\kappa,l}q_{\kappa'}u_{\kappa' y}{}^{l'}\left[\frac{\partial^2}{\partial y^2}\left(\frac{1}{r}\right)\right]_{r=r_{0\kappa'\kappa}{}^{l'l}}$$
$$-\sum_{\kappa',l'\neq\kappa,l}q_{\kappa'}u_{\kappa y}{}^{l}\left[\frac{\partial^2}{\partial y^2}\left(\frac{1}{r}\right)\right]_{r=r_{0\kappa'\kappa}{}^{l'l}} \quad \text{(A19)}$$

Using (A8), (A12), and (A13), the force on the κ, lth ion due to the dipolar field may be written

$$F_{\kappa y}{}^{l}=e^{-i\omega t}e^{2\pi i\mathbf{k}\cdot\mathbf{r}_{0\kappa l}}$$
$$\times\left\{\left(\sum_{\kappa'}\begin{bmatrix}\kappa & \kappa'\\ y & y\end{bmatrix}^{C}U_{\kappa' y}-\sum_{\kappa'}\begin{bmatrix}\kappa & \kappa'\\ y & y\end{bmatrix}^{C}_{k=0}U_{\kappa y}\right)\Big/\right.$$
$$\left.\left(1-\alpha\sum_{\kappa'}\frac{1}{q_\kappa q_{\kappa'}}\begin{bmatrix}\kappa & \kappa'\\ y & y\end{bmatrix}^{C}\right)\right\}. \quad \text{(A20)}$$

The equations of motion are

$$m_\kappa\omega^2U_{\kappa y}+\sum_{\kappa'}\begin{bmatrix}\kappa & \kappa'\\ y & y\end{bmatrix}^{R}U_{\kappa' y}-\sum_{\kappa'}\begin{bmatrix}\kappa & \kappa'\\ y & y\end{bmatrix}^{R}_{k=0}U_{\kappa y}$$
$$+\left\{\left(\sum_{\kappa'}\begin{bmatrix}\kappa & \kappa'\\ y & y\end{bmatrix}^{C}U_{\kappa' y}-\sum_{\kappa'}\begin{bmatrix}\kappa & \kappa'\\ y & y\end{bmatrix}^{C}_{k=0}U_{\kappa y}\right)\Big/\right.$$
$$\left.\left(1-\alpha\sum_{\kappa'}\frac{1}{q_\kappa q_{\kappa'}}\begin{bmatrix}\kappa & \kappa'\\ \nu & \nu\end{bmatrix}^{C}\right)\right\}=0. \quad \text{(A21)}$$

We have, however, neglected the force on the electronic dipole at the κ, lth site due to the interaction of this dipole with the fixed point-charge array. This will be taken into account now.

The y component of the force at a point κ', l' due to a dipole at κ, l is

$$q_{\kappa'} p_{\kappa y}{}^{l}\left[\frac{\partial^2}{\partial y^2}\left(\frac{1}{r}\right)\right]_{r=r_{0\kappa'\kappa}{}^{l'l}}. \tag{A22}$$

The force on the dipole due to the surrounding point charges is

$$-\sum_{\kappa',l'\neq\kappa,l} q_{\kappa'} p_{\kappa y}{}^{l}\left[\frac{\partial^2}{\partial y^2}\left(\frac{1}{r}\right)\right]_{r=r_{0\kappa'\kappa}{}^{l'l}} \tag{A23}$$

or using (A17)

$$-\alpha E \sum_{\kappa',l'\neq\kappa,l} q_{\kappa'} e^{2\pi i \mathbf{k}\cdot \mathbf{r}_{0\kappa l}}\left[\frac{\partial^2}{\partial y^2}\left(\frac{1}{r}\right)\right]_{r=r_{0\kappa'\kappa}{}^{l'l}}. \tag{A24}$$

Using Eq. (A20), we see that the equation of motion [Eq. (A21)] has the following term added to it:

$$-\alpha\sum_{\kappa'}\frac{1}{q_\kappa{}^2}\begin{bmatrix}\kappa & \kappa'\\ y & y\end{bmatrix}^{C}_{k=0} \times\left\{\left(\sum_{\kappa'}\begin{bmatrix}\kappa & \kappa'\\ y & y\end{bmatrix}^{C} U_{\kappa' y}-\sum_{\kappa'}\begin{bmatrix}\kappa & \kappa'\\ y & y\end{bmatrix}^{C} U_{\kappa y}\right)\Big/ \left(1-\alpha\sum_{\kappa'}\frac{1}{q_\kappa q_{\kappa'}}\begin{bmatrix}\kappa & \kappa'\\ y & y\end{bmatrix}^{C}\right)\right\}. \tag{A25}$$

The equation of motion can finally be written

$$m_\kappa\omega^2 U_{\kappa y}+\sum_{\kappa'}\begin{bmatrix}\kappa & \kappa'\\ y & y\end{bmatrix}^{R} U_{\kappa' y}-\sum_{\kappa'}\begin{bmatrix}\kappa & \kappa'\\ y & y\end{bmatrix}^{R}_{k=0} U_{\kappa y} +\left\{\left(1-\alpha\sum_{\kappa'}\frac{1}{q_\kappa{}^2}\begin{bmatrix}\kappa & \kappa'\\ y & y\end{bmatrix}^{C}_{k=0}\right)\Big/ \left(1-\alpha\sum_{\kappa'}\frac{1}{q_\kappa q_{\kappa'}}\begin{bmatrix}\kappa & \kappa'\\ y & y\end{bmatrix}^{C}\right)\right\} \times\left\{\sum_{\kappa'}\begin{bmatrix}\kappa & \kappa'\\ y & y\end{bmatrix}^{C} U_{\kappa' y}-\sum_{\kappa'}\begin{bmatrix}\kappa & \kappa'\\ y & y\end{bmatrix}^{C}_{k=0} U_{\kappa y}\right\}=0. \tag{A26}$$

The origin of the terms in Eq. (A26) are as follows. The first term is the inertial term. The second term arises from the short-range force on the κth ion due to the displacements from equilibrium of all other ions. The third term arises from the short-range force on the κth ion due to its displacement alone. The first term in the curly bracket arises from the Coulomb force on the κth ion due to the displacements of all other ions from equilibrium. The second term in this bracket arises from the Coulomb force on the κth ion due to its own displacement. Splitting up the forces in this fashion insures that we correctly calculate these forces at the displaced position of the κth ion. The effect of the introduction of polarizable ions appears as a quotient multiplying the curly bracket. The denominator arises from the contribution the surrounding electronic dipoles make to the local field at the κth site. The numerator arises from the force the κth electronic dipole experiences from the surrounding point charge array. This last contribution is not present in a diagonally cubic crystal.